# A LYST/beige homolog is involved in biogenesis of Dictyostelium secretory lysosomes

Charette, Steve; Cosson, Pierre

**How to cite**

CHARETTE, Steve, COSSON, Pierre. A LYST/beige homolog is involved in biogenesis of Dictyostelium secretory lysosomes. In: Journal of cell science, 2007, vol. 120, n° Pt 14, p. 2338–2343. doi: 10.1242/jcs.009001

This publication URL: https://archive-ouverte.unige.ch/unige:39513
Publication DOI: 10.1242/jcs.009001

# A LYST/beige homolog is involved in biogenesis of *Dictyostelium* secretory lysosomes

**Steve J. Charette* and Pierre Cosson**

Université de Genève, Centre Médical Universitaire, Département de Physiologie Cellulaire et Métabolisme, 1 rue Michel Servet, CH-1211 Geneva 4, Switzerland

*Author for correspondence (e-mail: steve.charette@medecine.unige.ch)

*Accepted 10 May 2007*
*Journal of Cell Science 120, 2338-2343 Published by The Company of Biologists 2007*
*doi:10.1242/jcs.009001*

## Summary

**Chediak-Higashi syndrome (CHS) is characterized at the cellular level by a defect in the ability of cells to secrete lysosomes. However, the precise step affected in the secretion process is unclear. We characterized *Dictyostelium discoideum* cells containing a mutation in *lvsB*, the homolog of the human gene (*LYST*) involved in CHS. As observed in mammalian cells, secretion of lysosome-derived compartments was affected in *lvsB* mutant cells. This defect was mirrored by a decrease in the number of fusion-competent post-lysosomal compartments, which in *Dictyostelium* can be clearly distinguished from lysosomes. In addition, the transfer of endocytosed particles from lysosomes to post lysosomes was strongly diminished in *lvsB* mutant cells compared with the wild type. These results suggest that LvsB is primarily involved in transport from lysosomes to post lysosomes, and thus plays a critical role in the maturation of lysosomes into fusion-competent post-lysosomal compartments.**

Supplementary material available online at
http://jcs.biologists.org/cgi/content/full/120/14/2338/DC1

Key words: Lysosome, Exocytosis, Chediak-Higashi syndrome, Beige, LvsB, *Dictyostelium discoideum*

## Introduction

In eukaryotic cells, endocytosed material is delivered to acidic membrane-delimited lysosomes where it is degraded by specific enzymes. In some specialized cells, a subpopulation of lysosomes can mature into secretory lysosomes capable of fusing with the cell surface. Exocytosis of these specialized lysosomes plays a key role in a number of essential physiological events such as the immune response (for reviews, see Holt et al., 2006; Stinchcombe et al., 2004). Exocytosis of conventional lysosomes can also be induced in non-specialized cell types and might participate notably in the repair of plasma membrane lesions (Andrews, 2000; McNeil and Steinhardt, 2003). Alterations in lysosome secretion lead to severe health problems in a few genetic diseases, revealing the role of a collection of proteins in lysosome secretion (reviewed by Holt et al., 2006). Technical limitations have made it difficult to define the exact role of various proteins in lysosome exocytosis, notably the fact that lysosome exocytosis is a transient event that is difficult to visualize. Since no marker specific for fusion-competent lysosomes has been characterized, it is also difficult to determine whether a block in lysosome secretion is caused by an inhibition of the fusion process, or by a defective biogenesis of fusion-competent post lysosomes.

*Dictyostelium discoideum* amoebae have been used previously to study the function of the endocytic pathway. In these cells, endocytosed material reaches rapidly acidic compartments filled with lysosomal enzymes and delimited by a membrane exhibiting $H^+$-ATPase (Fig. 1A). Lysosomes then mature into neutral compartments (Padh et al., 1993) devoid of $H^+$-ATPase and enriched in the p80 protein (Ravanel et al., 2001). These compartments are called post lysosomes in *Dictyostelium* (Fig. 1A) and are functionally equivalent to mammalian fusion-competent lysosomes. Actin also accumulates specifically on the cytoplasmic face of post-lysosomal compartments (Rauchenberger et al., 1997). Owing to their large diameter (about 2 μm), the fusion of post lysosomes with the cell surface can also be observed and quantified relatively easily (Charette and Cosson, 2006). In addition, specific knockout mutants can be generated relatively readily in *Dictyostelium*, making this a unique model to determine the precise stage at which various proteins are implicated in the secretion of post lysosomes.

Chediak-Higashi syndrome (CHS) was first described 60 years ago (Beguez-Cesar, 1943; Chediak, 1952; Higashi, 1954). It is a rare autosomal recessive disorder that is accompanied by severe symptoms including immunological defects, which often lead to death. In specialized cells, such as cytotoxic T cells from CHS patients, lysosomes formed during differentiation are enlarged and are not secreted upon stimulation, although their content is apparently normal (Baetz et al., 1995). Non-specialized CHS cells also present enlarged lysosomes, which fail to fuse efficiently with the cell surface in response to membrane lesions (Huynh et al., 2004). The gene mutated in patients with CHS encodes a protein named lysosomal trafficking regulator or LYST (previously known as CHS1 in human and beige in mouse) (Barbosa et al., 1996; Nagle et al., 1996; Perou et al., 1996). The exact role of LYST in the biology of lysosomes is still unclear. It has previously been shown that mutants in *lvsB*, the *Dictyostelium* homolog

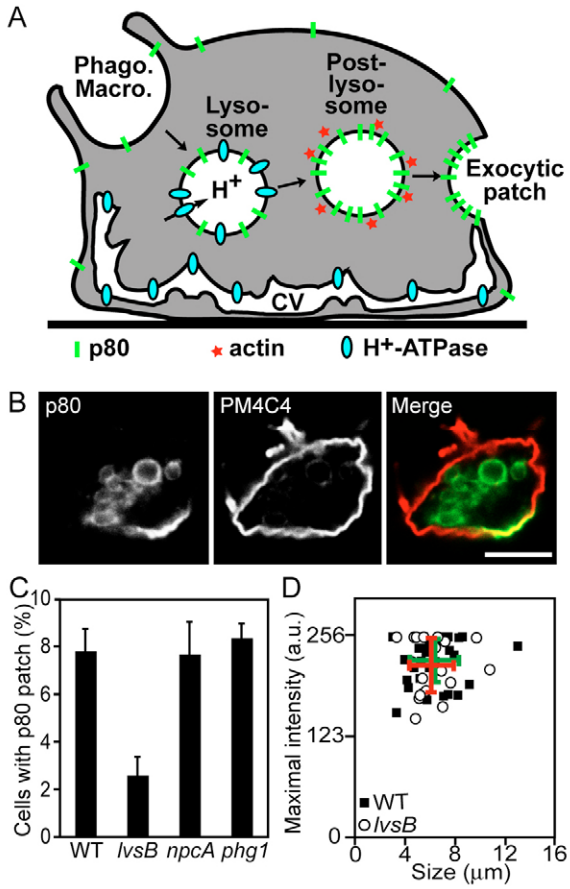


**Fig. 1.** Defective secretion of post lysosomes in *lvsB* mutant cells. (A) Schematic representation of the endocytic pathway in *Dictyostelium.* Phagocytosis and macropinocytosis allow internalization of extracellular material into acidic lysosomes. These compartments then mature into neutral post lysosomes, which are eventually exocytosed. The contractile vacuole (CV) is a non-endocytic specialized organelle involved in osmoregulation. The localization of the different markers (p80, $H^+$-ATPase and actin) used in this study is shown. (B) Confocal images of a typical exocytic p80 patch at the cell surface. Cells were fixed and stained for p80 (green) and PM4C4 (red). The PM4C4 protein is evenly distributed at the plasma membrane whereas p80 is highly concentrated in exocytic patches at the cell surface. Bar, 5 µm. (C) Fewer p80 patches in *lvsB* mutant cells. The percentage of cells exhibiting a surface p80 patch was determined for each cell line. The mean and s.e.m. of three independent experiments are indicated. At least 300 cells were analyzed for each cell type in each experiment. (D) The p80 patches found at the surface of *lvsB* mutant cells are similar in size and intensity to those found in WT cells. Exocytic p80 patches were identified on random confocal images, and for each patch the size and the intensity of p80 fluorescence were determined. Twenty patches were analyzed for WT and *lvsB* mutant cells. Each dot represents one patch and colored crosses indicate the average size and intensity as well as the s.d. of the results (green, WT; red, *lvsB*).

of the *LYST* gene recapitulate several features of the Chediak-Higashi syndrome in *Dictyostelium* cells (Wang et al., 2002), notably an enlargement of endocytic compartments, and anomalies in the secretion of lysosomal enzymes (Cornillon et al., 2002; Harris et al., 2002; Marchetti et al., 2004). Here we show that the *Dictyostelium* LvsB protein is specifically involved in the biogenesis of fusion-competent post-lysosomal compartments.

## Results

### Decreased secretion of post lysosomes in *lvsB* mutant cells

*Dictyostelium* post lysosomes are a distinct endocytic compartment capable of fusing with the cell surface, and thus represent the equivalent of fusion-competent secretory lysosomes in mammalian cells. The fusion of post lysosomes with the cell surface results in the transient formation of a microdomain at the cell surface characterized by a high concentration of p80, a transmembrane protein abundant in post lysosomes (Charette and Cosson, 2006) (Fig. 1A,B). Since p80 patches are very intense, their presence at the surface of cells can be easily assessed by examining labeled cells. The proportion of cells exhibiting p80-rich microdomains was thus used to evaluate the capacity of different mutant cells to secrete post lysosomes. In addition to *lvsB* mutant cells, cells mutated for the *phg1* and *npcA* genes were also tested. Phg1 has been implicated in the function of the endocytic pathway in *Dictyostelium* based notably on the observation that *phg1* mutant cells displayed an altered array of membrane protein at their surface (Benghezal et al., 2003). NpcA is the *Dictyostelium* ortholog of human NPC1, which is also involved in the function of endosomes in human cells (Chang et al., 2005). As shown in Fig. 1C, only *lvsB* mutant cells presented a decreased number of exocytic patches compared with the wild type (WT) (33±8% of WT, mean ± s.d. of nine experiments; $P<0.01$), suggesting that, as observed in cells of patients with CHS, post-lysosome exocytosis is decreased in *lvsB* mutant cells.

To analyze the size and intensity of p80 patches in both WT and *lvsB* mutant cells, we performed a quantitative analysis of confocal images. Only the number of exocytic patches was affected in *lvsB* mutant cells; the size and intensity of the p80 patches were equivalent in WT and *lvsB* mutant cells (Fig. 1D). To establish the specificity of the defect observed in *lvsB* mutant cells, other plasma membrane markers (p25, H36, PM4C4) were analyzed, and no alteration in their localization was noticed in *lvsB* mutant cells compared with WT cells (see supplementary material Fig. S1).

### Decreased number of post lysosomes in *lvsB* mutant cells

The reduced number of exocytic events in *lvsB* mutant cells might be the consequence of a deficiency in the fusion process per se or reflect a biogenesis defect of fusion-competent compartments. The first situation (fusion defect) should result in an increase of fusion-competent post lysosomes, whereas the second situation (biogenesis defect) would cause a decrease in the number of post lysosomes. Post lysosomes contain p80, but lack $H^+$-ATPase and can be thus easily distinguished from p80-positive, $H^+$-ATPase-positive lysosomes (Fig. 1A, Fig. 2A). When analyzed by immunofluorescence, *lvsB* mutant cells displayed a markedly reduced number of post lysosomes compared with WT cells (45±9% of WT, mean ± s.d. of three experiments; $P<0.01$) or to other mutant cells tested (Fig. 2B,C). The size of post lysosomes was similar in all cells (Fig. 2D).

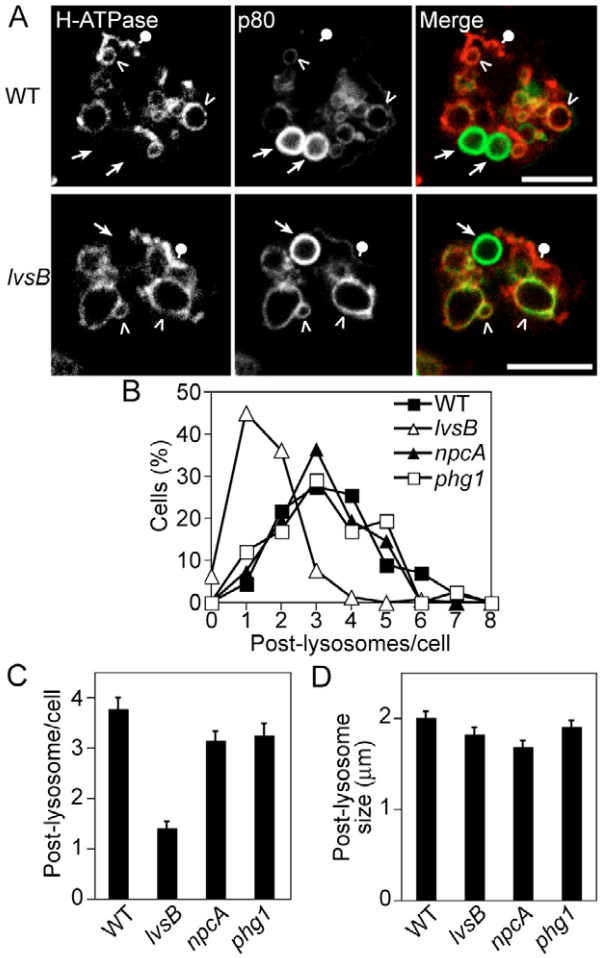


**Fig. 2.** The *lvsB* mutant cells contain fewer H$^+$-ATPase-negative post lysosomes. (A) Lysosomes (p80-positive, H$^+$-ATPase-positive; arrowheads) and post lysosomes (p80-positive, H$^+$-ATPase-negative; arrows) were identified by double immunofluorescence. The compartments positive for H$^+$-ATPase but negative for p80 represent contractile vacuoles (pinhead). Bars, 5 μm. (B,C) A decreased number of post lysosomes was found in *lvsB* mutant cells. To determine the number of post lysosomes (defined as p80-positive and H$^+$-ATPase-negative vacuoles), cells were scanned from bottom (attached to the substratum) to top, and post lysosomes were counted. In B, the percentage of cells with a given number of post lysosomes is indicated. (D) The size of post lysosomes was similar in mutant and WT cells. All experiments were repeated three times with equivalent results. One representative set of data is shown in B. Means + s.e.m. are shown in C and D.

The size and number of lysosomes was also determined in random confocal pictures of cells stained for both H$^+$-ATPase and p80. The diameter of lysosomes in *lvsB* mutant cells was 27% larger than in WT cells (see Table 1), corroborating previous observations (Harris et al., 2002; Marchetti et al., 2004), but their number was reduced by 28%. Overall the total surface of lysosomal compartments was 23% higher in *lvsB* than in WT cells (Table 1). Interestingly, the total membrane area for lysosomes plus post lysosomes was the same in the two cell types.

Post-lysosomal compartments can also be distinguished from lysosomes based on the accumulation of actin on their cytosolic face (Rauchenberger et al., 1997) (Fig. 1A, Fig. 3A). Using actin staining to identify post lysosomes, we also observed that the number of post lysosomes in *lvsB* mutant cells was reduced markedly compared with WT cells (Fig. 3B). To establish the degree of overlap between these two ways of identifying post lysosomes (absence of H$^+$-ATPase or presence of actin on p80-positive vacuoles), WT and *lvsB* mutant cells were stained for the three markers (p80, actin and H$^+$-ATPase). The analysis of these cells revealed that in both WT and *lvsB* mutant cells, 95% of the p80 vacuoles decorated with actin were H$^+$-ATPase-negative (Fig. 4). The decreased number of post lysosomes in *lvsB* mutant cells suggests that the defect in post-lysosome secretion is mostly caused by a defect in the formation of post lysosomes in these cells. Moreover, our results suggest that post lysosomes in *lvsB* mutant cells have retained the characteristics (p80-positive, actin-positive and H$^+$-ATPase-negative) seen in WT cells.

### Defective lysosome maturation in *lvsB* mutant cells

The results presented above suggested that the maturation of lysosomes into post lysosomes was defective in *lvsB* mutant cells. If true, this hypothesis would also predict a slower transfer of endocytosed material from lysosomes to post lysosomes. This can be assessed precisely in *Dictyostelium* cells by following the maturation of endocytic compartments containing internalized fluorescent particles. In WT cells, internalized latex beads were found in lysosomal compartments after 30 minutes (p80-positive, H$^+$-ATPase-positive) (data not shown). They were then gradually transferred to post-lysosomal compartments (p80-positive, H$^+$-ATPase-negative) after 60 and 90 minutes (Fig. 5). In *lvsB* mutant cells, transfer of particles to post-lysosomal compartments was markedly slower (Fig. 5), suggesting that maturation of lysosomes into post lysosomes was slower than in WT cells. Analysis of longer chase times was difficult, because WT cells exocytosed efficiently phagocytosed beads after 90 minutes (data not shown).

**Table 1. Lysosomes (Ly) and post lysosomes (PL) in WT and *lvsB* mutant cells***

| | Diameter (μm) | | Area (μm$^2$)$^\dagger$ | | Number of vacuoles/ confocal image | | Total area/ confocal image (μm$^2$) | | Total area (Ly+PL) (μm$^2$) |
|---|---|---|---|---|---|---|---|---|---|
| Cells | Ly | PL | Ly | PL | Ly | PL | Ly | PL | |
| WT | 1.16±0.01 | 1.75±0.07 | 4.65±0.13 | 10.32±0.93 | 11.44±0.26 | 2.61±0.07 | 53.21±1.37 | 26.84±1.78 | 80.05±2.03 |
| *lvsB* | 1.47±0.04 | 1.88±0.08 | 8.01±0.50 | 11.84±0.99 | 8.19±0.34 | 1.24±0.05 | 65.26±1.36 | 14.56±0.65 | 79.82±1.98 |

*Analysis was performed as described in the Materials and Methods. It was repeated on three different sets of images. Each set comprised at least 17 images of WT and *lvsB* mutant cells. The values are means of these three experiments (± s.e.m.).

$^\dagger$To calculate the surface area of lysosomes and post lysosomes they were assumed to be spherical (Surface area=$\pi d^2$).

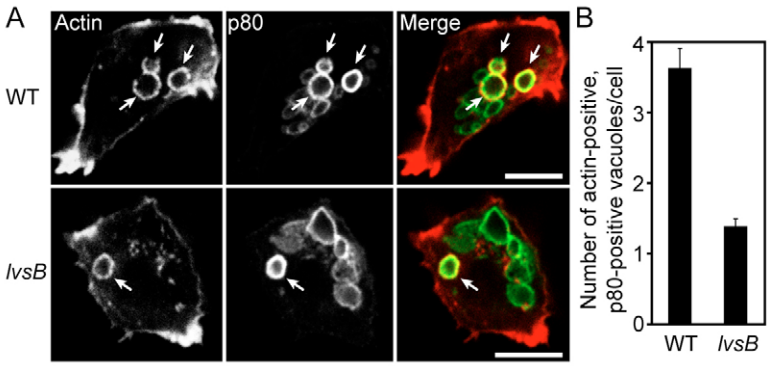


**Fig. 3.** A reduced number of actin-positive post lysosomes were observed in *lvsB* mutant cells. (A) Post lysosomes were identified by immunofluorescence as p80-positive and actin-positive compartments (arrows). Bars, 5 μm. (B) Fewer actin- and p80-positive vacuoles were observed in *lvsB* mutant cells. The means + s.e.m. of three independent experiments are indicated. At least 30 cells were analyzed for each cell type in each experiment.

The p80 endosomal marker is continuously delivered to the cell surface by the fusion of post lysosomes (Charette and Cosson, 2006). At the cell surface, macropinosomes forming continuously contain p80 at a concentration similar to that found at the cell surface, accounting for its rapid endocytosis (Mercanti et al., 2006). P80 then concentrates gradually in lysosomes, and then in post lysosomes (Ravanel et al., 2001) (Fig. 1A). In a mutant where transfer to post lysosomes is affected, this cycle should be perturbed. In *lvsB* mutant cells, the total amount of p80 was similar to that found in WT cells, as assessed by immunoblotting (Fig. 6A). However, the amount of p80 present at the cell surface was lower than in WT cells (62±9% of WT, after subtraction of the background, mean ± s.d. of three different experiments, Fig. 6B) whereas the surface concentration of p25, another plasma membrane marker (Ravanel et al., 2001), was identical in both cell types (Fig. 6B). By contrast, the concentration of p80 in lysosomes, determined by immunofluorescence, was higher in *lvsB* mutant cells than in WT cells (Fig. 6C). Similar p80 concentrations were observed in post lysosomes from both mutant and WT cells (Fig. 6C insert). This change in the equilibrium distribution of p80 in *lvsB* mutant cells was not due to an alteration of the endocytosis of p80: as in WT cells, p80 was present at a similar concentration at the cell surface and in forming macropinosomes (Fig. 6D). Together these results suggest that in *lvsB* mutant cells, the transport of p80 from lysosomes to post lysosomes is slowed down, a result compatible with the notion that biogenesis of post lysosomes is diminished.

## Discussion

In this study, we took advantage of the many specific tools and protocols that have been developed recently to study the endocytic pathway in *Dictyostelium* cells and we investigated the nature of the defect observed in *lvsB* mutant cells. Our results indicated that, similarly to that observed in human CHS cells, fusion of post lysosomes to the cell surface is significantly reduced in *lvsB* mutant cells compared with WT cells. Remarkably, this decrease in post-lysosome fusion was accompanied by a quantitatively similar decrease in the number of fusion-competent post lysosomes. Although the fusion efficacy of individual post lysosomes was technically difficult to assess, the simplest interpretation of these observations is that the decrease in post-lysosome fusion in *lvsB* mutant cells is solely caused by the decrease in their absolute number. Two lines of evidence further suggest a defect in the biogenesis of post lysosomes in *lvsB* mutant cells: first, transfer of internalized particles from lysosomes to post lysosomes is markedly slower in *lvsB* mutant cells than in WT cells; second, in *lvsB* mutant cells, p80 is depleted from the cell surface and concentrated in lysosomal compartments, suggesting that the transfer of p80 to post lysosomes is diminished. Further experiments will be necessary to determine whether abnormal maturation of lysosomes is caused by their abnormal fusion properties (Harris et al., 2002).

The interpretation of our observations was made possible primarily because *lvsB* mutant cells presented relatively limited and specific alterations compared with WT cells. In particular

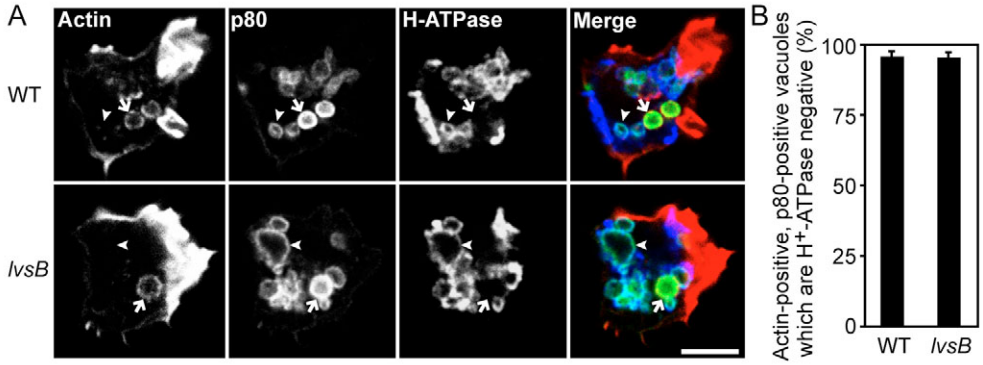


**Fig. 4.** Endosomal $H^+$-ATPase and actin are mutually exclusive. (A) Actin was present only on vacuoles stained for p80 but not for $H^+$-ATPase (post lysosomes, arrows). Conversely, actin was not observed on vacuoles positive for both p80 and $H^+$-ATPase (lysosomes, arrowheads). Bar, 5 μm. (B) Percentage of the p80-positive, actin-positive vacuoles containing no $H^+$-ATPase. The means + s.e.m. of three independent experiments are indicated. All the p80-positive, actin-positive vacuoles of at least 30 cells were analyzed for each cell type in each experiment.

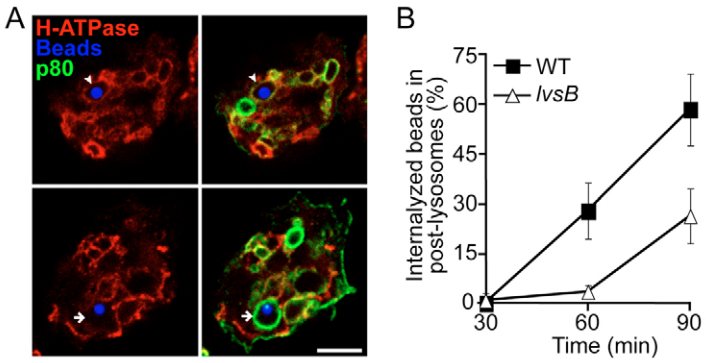


**Fig. 5.** Delayed lysosome maturation in *lvsB* mutant cells. Cells were allowed to internalize 1-μm-diameter latex beads for 15 minutes, washed to remove non-internalized beads and incubated further for 15, 45 and 75 minutes (for a total incubation time of 30, 60 or 90 minutes), fixed and processed for immunofluorescence to detect p80 and $H^+$-ATPase. (A) Typical images of internalized beads present in lysosomes ($H^+$-ATPase-positive, p80-positive vacuoles; top picture; arrowhead) and in post lysosomes ($H^+$-ATPase-negative, p80-positive vacuoles; bottom picture; arrow). Bar, 5 μm. (B) The percentage of internalized beads found in post lysosomes was determined. The curves show the means ± s.e.m. of three experiments. Forty cells containing internalized beads were analyzed for each cell type and at each time point in each experiment

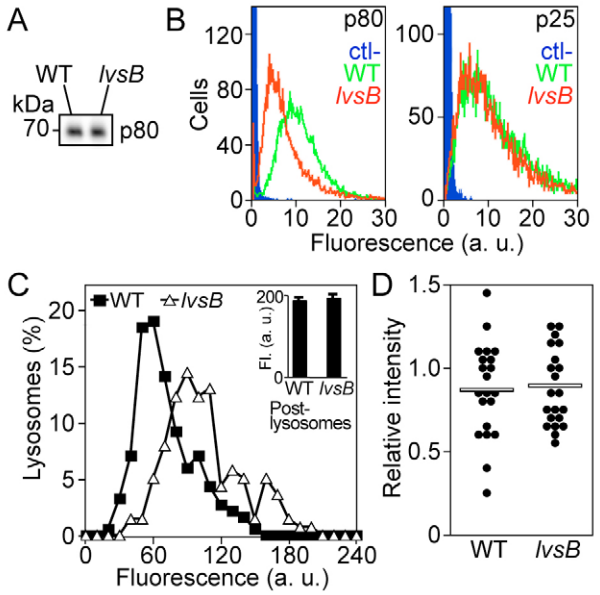


**Fig. 6.** Defect in protein transfer from lysosomes to post lysosomes in *lvsB* mutant cells. (A) The p80 protein is expressed at the same level in WT and *lvsB* mutant cells as shown by immunoblot analysis. For both cell lines, the total lysate from 125,000 cells was loaded on an electrophoresis gel, migrated, transferred to nitrocellulose and revealed with an antibody to p80. (B) The p80 protein is present at a lower level at the cell surface of *lvsB* mutant cells compared with WT cells as determined by FACS analysis of surface-labeled cells. No alteration in the surface level of p25 was seen in *lvsB* mutant cells. A negative control (ctl-) is also shown (first antibody omitted). (C) The p80 protein is more concentrated in the lysosomes of *lvsB* mutant cells, but normally distributed in post lysosomes. The p80 intensity in lysosomes of WT and *lvsB* mutant cells is shown. Insert, mean + s.e.m. of p80 intensity in post lysosomes. Quantification was done as described in the Materials and Methods to allow direct comparison of p80 intensities in both cell types. (D) Internalization of p80 in macropinosomes is equivalent in WT and *lvsB* mutant cells. Each dot represents the relative intensity of the p80 protein in a CRAC-GFP-positive macropinosome compared with the cell surface. The means are indicated by bars. The experiments shown in B, C and D were repeated three times with equivalent results and one representative set of data is shown.

the size of post lysosomes, the accumulation of p80 in post lysosomes, the internalization of p80 in macropinosomes, the total p80 expression level and the size and intensity of p80 microdomains were all similar in WT and *lvsB* mutant cells. Moreover we also observed that there was no mislocalization of actin on lysosome ($H^+$-ATPase-positive vacuoles) in *lvsB* mutant cells. These data all suggest that LvsB plays a specific role in post-lysosome biogenesis but not in the compartmentalization of the endocytic pathway. This is compatible with a previous report on cytotoxic T cells from CHS patients where lysosomal markers, such as granzyme A, cathepsin D and mannose-6-phosphate receptor were properly localized (Baetz et al., 1995).

By combining precise analytical tools and the ability to generate specific mutants, this system will be particularly interesting in the future to determine how a number of other mutations affect the secretion of lysosomes. This might provide a more precise view of the role of various gene products in the endocytic pathway of eukaryotic cells, and lead to a better understanding of the cellular defects observed in patients suffering from a number of genetic diseases affecting the endocytic pathway.

## Materials and Methods

### Cells and reagents

*Dictyostelium* cells were grown at 21°C in HL5 medium (Mercanti et al., 2006). All strains used in this study were derived from the subclone DH1-10 (Cornillon et al., 2000) of the *D. discoideum* WT strain DH1 (Caterina et al., 1994). Knockout cells for *lvsB* and *phg1* were described previously (Cornillon et al., 2002; Cornillon et al., 2000). NpcA is the *Dictyostelium* ortholog of the human NPC1 (Chang et al., 2005) as determined by the DictyBase group (Chisholm et al., 2006). *NpcA* knockout cells were generated as described in supplementary material Fig. S2. Cells constitutively expressing the PH domain of cytosolic regulator of adenylylcyclase fused to green fluorescent protein (CRAC-GFP) were generated as described previously (Mercanti et al., 2006).

Mouse monoclonal antibodies against the p80 endosomal marker (H161), p25 (H72) and the plasma membrane proteins PM4C4 (V4C4F3) and H36 (H36) were described previously (Ravanel et al., 2001; Schwarz et al., 2000; Mercanti et al., 2006). 221-35-2 is a mouse monoclonal antibody recognizing vacuolar $H^+$-ATPase (Neuhaus et al., 1998) and was a kind gift from G. Gerisch (Max-Planck-Institute, Martinsried, Germany). Actin cytoskeleton was labeled using TRITC-phalloidin (Sigma, St Louis, MO).

### Immunofluorescence

Cells ($0.5\times10^6$) were allowed to attach on a glass coverslip in fresh HL5 medium for 3 hours at 21°C and then fixed, permeabilized and labeled as described (Charette and Cosson, 2006). Cells were permeabilized by incubation in phosphate buffer containing 0.1% saponin when the actin cytoskeleton was stained. Cells were visualized with an LSM510 confocal microscope (Carl Zeiss, Feldbach, Switzerland).

To determine the kinetics of lysosome maturation, cells plated on a coverslip were incubated with FITC 1 μm-diameter latex beads (Polysciences, Warrington, PA) for 15 minutes, washed three times with HL5 medium and then incubated for various periods of time before fixation. Fixed cells were processed for immunofluorescence as described above to detect both the $H^+$-ATPase and p80 proteins.

To measure the presence of the p80 protein in macropinosomes, WT and *lvsB* mutant cells expressing CRAC-GFP, a marker that accumulates on the cytosolic face

of newly formed macropinosomes, were fixed and immunostained to detect the p80 protein. The quantification of the p80 protein in macropinosomes and at the cell surface was done as described (Mercanti et al., 2006).

### Image analysis

To determine the number of post lysosomes (defined either as p80-positive and $H^+$-ATPase-negative vacuoles or as p80-positive and actin-positive vacuoles) in each cell, confocal imaging was used to scan cells from their basal part (attached to the substratum) up to the top and vacuoles corresponding to these criteria were counted. The size of post lysosomes was determined using the 'Profile' tool of the LSM510 confocal microscope software.

To measure the size of lysosomes and post lysosomes, random confocal images of cells stained for both $H^+$-ATPase and p80 were taken for both WT and *lvsB* mutant cells. On each image, the diameter of all discernible lysosomes ($H^+$-ATPase-positive and p80-positive vacuoles) and post lysosomes ($H^+$-ATPase-negative, p80-positive vacuoles) was measured using the linescan tool of the Metamorph 6.0 software (Universal Imaging Corporation, Downingtown, PA).

For the quantitative analysis of p80 intensity in both exocytic microdomain and lysosomes, the Metamorph 6.0 software was used. Confocal images of fixed cells immunostained for the p80 protein were acquired randomly and consecutively using the same laser and software set-ups to allow direct comparison of fluorescence intensities. Laser intensity was adjusted at the beginning to obtain images where the p80 intensity of the brightest structures (the post lysosomes) was just below saturation (i.e. an intensity level of 256 arbitrary units). Using this protocol, a preliminary analysis led us to define p80 patches as a surface area extending over at least 2.5 μm with an intensity reaching at least 150 arbitrary units. These criteria were then used to compare the characteristics of p80 patches in WT or *lvsB* mutant cells. Twenty patches in each cell type were randomly identified and their size and maximal intensity were determined using the line-scan tool of Metamorph 6.0 software. The intensity of the p80 labeling decreased sharply at the border between the patch and the rest of the plasma membrane, allowing the possibility to determine unambiguously the size of each patch.

To analyze the p80 labeling intensity in lysosomes and post lysosomes, cells were co-stained for p80 and $H^+$-ATPase and images of 20 different cells for both WT and *lvsB* mutant cells were acquired randomly as described above. The compartments were identified based on the presence (lysosomes) or absence (post lysosomes) of $H^+$-ATPase labeling. The average p80 fluorescence intensity of the region corresponding to the membrane of each compartment was determined. About 200 compartments were analyzed for each cell type in each experiment.

### Quantification of the p80 protein present at the cell surface

To quantify the amount of p80 protein at the cell surface, cells plated on a coverslip were incubated at 4°C with the H161 antibody in HL5 containing 0.1% $NaN_3$ for 10 minutes. The cells were then washed and incubated still at 4°C with a secondary antibodies directed against mouse IgG and coupled to Alexa Fluor 647. Finally cells were washed, resuspended and analyzed in a fluorescence-activated cell sorter (FACSCalibur, Becton-Dickinson, San Jose, CA) to measure the cell surface-associated fluorescence.

### Protein electrophoresis and immunodetection

The total amount of p80 in cells was determined by standard protein electrophoresis and immunodetection methods as already described (Mercanti et al., 2006) using the H161 antibody.

We thank Patricia Halls, François Letourneur and Valentina Mercanti for critical reading of the manuscript. This work was supported by the Fonds National Suisse de la Recherche Scientifique (to P.C.). The P.C. research group participates in the NEMO network, supported by the 3R Foundation. S.J.C. received fellowships from the Human Frontier Science Program and the Fondation Ernst et Lucie Schmidheiny.

## References

**Andrews, N. W.** (2000). Regulated secretion of conventional lysosomes. *Trends Cell Biol.* **10**, 316-321.

**Baetz, K., Isaaz, S. and Griffiths, G. M.** (1995). Loss of cytotoxic T lymphocyte function in Chediak-Higashi syndrome arises from a secretory defect that prevents lytic granule exocytosis. *J. Immunol.* **154**, 6122-6131.

**Barbosa, M. D., Nguyen, Q. A., Tchernev, V. T., Ashley, J. A., Detter, J. C., Blaydes, S. M., Brandt, S. J., Chotai, D., Hodgman, C., Solari, R. C. et al.** (1996). Identification of the homologous beige and Chediak-Higashi syndrome genes. *Nature* **382**, 262-265.

**Beguez-Cesar, A. B.** (1943). Neutropenia cronica maligna familiar con. *Bol. Soc. Cubana Pediatr.* **15**, 920-922.

**Benghezal, M., Cornillon, S., Gebbie, L., Alibaud, L., Bruckert, F., Letourneur, F. and Cosson, P.** (2003). Synergistic control of cellular adhesion by transmembrane 9 proteins. *Mol. Biol. Cell* **14**, 2890-2899.

**Caterina, M. J., Milne, J. L. and Devreotes, P. N.** (1994). Mutation of the third intracellular loop of the cAMP receptor, cAR1, of Dictyostelium yields mutants impaired in multiple signaling pathways. *J. Biol. Chem.* **269**, 1523-1532.

**Chang, T. Y., Reid, P. C., Sugii, S., Ohgami, N., Cruz, J. C. and Chang, C. C.** (2005). Niemann-Pick type C disease and intracellular cholesterol trafficking. *J. Biol. Chem.* **280**, 20917-20920.

**Charette, S. J. and Cosson, P.** (2006). Exocytosis of late endosomes does not directly contribute membrane to the formation of phagocytic cups or pseudopods in Dictyostelium. *FEBS Lett.* **580**, 4923-4928.

**Chediak, M.** (1952). Nouvelle anomalie leucocytaire de caractère constitutionnel et familial. *Rev. Hematol.* **7**, 362-367.

**Chisholm, R. L., Gaudet, P., Just, E. M., Pilcher, K. E., Fey, P., Merchant, S. N. and Kibbe, W. A.** (2006). dictyBase, the model organism database for Dictyostelium discoideum. *Nucleic Acids Res.* **34**, D423-D427.

**Cornillon, S., Pech, E., Benghezal, M., Ravanel, K., Gaynor, E., Letourneur, F., Bruckert, F. and Cosson, P.** (2000). Phg1p is a nine-transmembrane protein superfamily member involved in dictyostelium adhesion and phagocytosis. *J. Biol. Chem.* **275**, 34287-34292.

**Cornillon, S., Dubois, A., Bruckert, F., Lefkir, Y., Marchetti, A., Benghezal, M., De Lozanne, A., Letourneur, F. and Cosson, P.** (2002). Two members of the beige/CHS (BEACH) family are involved at different stages in the organization of the endocytic pathway in Dictyostelium. *J. Cell Sci.* **115**, 737-744.

**Harris, E., Wang, N., Wu, W.-I., Weatherford, A., De Lozanne, A. and Cardelli, J.** (2002). Dictyostelium LvsB mutants model the lysosomal defects associated with Chediak-Higashi syndrome. *Mol. Biol. Cell* **13**, 656-669.

**Higashi, O.** (1954). Congenital gigantism of peroxidase granules; the first case ever reported of qualitative abnormity of peroxidase. *Tohoku J. Exp. Med.* **59**, 315-332.

**Holt, O. J., Gallo, F. and Griffiths, G. M.** (2006). Regulating secretory lysosomes. *J. Biochem.* **140**, 7-12.

**Huynh, C., Roth, D., Ward, D. M., Kaplan, J. and Andrews, N. W.** (2004). Defective lysosomal exocytosis and plasma membrane repair in Chediak-Higashi/beige cells. *Proc. Natl. Acad. Sci. USA* **101**, 16795-16800.

**Marchetti, A., Mercanti, V., Cornillon, S., Alibaud, L., Charette, S. J. and Cosson, P.** (2004). Formation of multivesicular endosomes in Dictyostelium. *J. Cell Sci.* **117**, 6053-6059.

**McNeil, P. L. and Steinhardt, R. A.** (2003). Plasma membrane disruption: repair, prevention, adaptation. *Annu. Rev. Cell Dev. Biol.* **19**, 697-731.

**Mercanti, V., Charette, S. J., Bennett, N., Ryckewaert, J. J., Letourneur, F. and Cosson, P.** (2006). Selective membrane exclusion in phagocytic and macropinocytic cups. *J. Cell Sci.* **119**, 4079-4087.

**Nagle, D. L., Karim, M. A., Woolf, E. A., Holmgren, L., Bork, P., Misumi, D. J., McGrail, S. H., Dussault, B. J., Jr, Perou, C. M., Boissy, R. E. et al.** (1996). Identification and mutation analysis of the complete gene for Chediak-Higashi syndrome. *Nat. Genet.* **14**, 307-311.

**Neuhaus, E. M., Horstmann, H., Almers, W., Maniak, M. and Soldati, T.** (1998). Ethane-freezing/methanol-fixation of cell monolayers: a procedure for improved preservation of structure and antigenicity for light and electron microscopies. *J. Struct. Biol.* **121**, 326-342.

**Padh, H., Ha, J., Lavasa, M. and Steck, T. L.** (1993). A post-lysosomal compartment in Dictyostelium discoideum. *J. Biol. Chem.* **268**, 6742-6747.

**Perou, C. M., Moore, K. J., Nagle, D. L., Misumi, D. J., Woolf, E. A., McGrail, S. H., Holmgren, L., Brody, T. H., Dussault, B. J., Jr, Monroe, C. A. et al.** (1996). Identification of the murine beige gene by YAC complementation and positional cloning. *Nat. Genet.* **13**, 303-308.

**Rauchenberger, R., Hacker, U., Murphy, J., Niewohner, J. and Maniak, M.** (1997). Coronin and vacuolin identify consecutive stages of a late, actin-coated endocytic compartment in Dictyostelium. *Curr. Biol.* **7**, 215-218.

**Ravanel, K., de Chassey, B., Cornillon, S., Benghezal, M., Zulianello, L., Gebbie, L., Letourneur, F. and Cosson, P.** (2001). Membrane sorting in the endocytic and phagocytic pathway of Dictyostelium discoideum. *Eur. J. Cell Biol.* **80**, 754-764.

**Schwarz, E. C., Neuhaus, E. M., Kistler, C., Henkel, A. W. and Soldati, T.** (2000). Dictyostelium myosin IK is involved in the maintenance of cortical tension and affects motility and phagocytosis. *J. Cell Sci.* **113**, 621-633.

**Stinchcombe, J., Bossi, G. and Griffiths, G. M.** (2004). Linking albinism and immunity: the secrets of secretory lysosomes. *Science* **305**, 55-59.

**Wang, N., Wu, W.-I. and De Lozanne, A.** (2002). BEACH family of proteins: phylogenetic and functional analysis of six Dictyostelium BEACH proteins. *J. Cell. Biochem.* **86**, 561-570.